

RESEARCH

Open Access



Regional differences in synaptic degeneration are linked to alpha-synuclein burden and axonal damage in Parkinson's disease and dementia with Lewy bodies

Irene Frigerio^{1,2,3*} , Maud M. A. Bouwman^{1,2,3}, Ruby T. G. M. M. Noordermeer¹, Ema Podobnik¹, Marko Popovic⁴, Evelien Timmermans¹, Annemieke J. M. Rozemuller⁵, Wilma D. J. van de Berg^{1,2} and Laura E. Jonkman^{1,2,3}

Abstract

Regional differences in synaptic degeneration may underlie differences in clinical presentation and neuropathological disease progression in Parkinson's Disease (PD) and Dementia with Lewy bodies (DLB). Here, we mapped and quantified synaptic degeneration in cortical brain regions in PD, PD with dementia (PDD) and DLB, and assessed whether regional differences in synaptic loss are linked to axonal degeneration and neuropathological burden. We included a total of 47 brain donors, 9 PD, 12 PDD, 6 DLB and 20 non-neurological controls. Synaptophysin⁺ and SV2A⁺ puncta were quantified in eight cortical regions using a high throughput microscopy approach. Neurofilament light chain (NfL) immunoreactivity, Lewy body (LB) density, phosphorylated-tau and amyloid- β load were also quantified. Group differences in synaptic density, and associations with neuropathological markers and Clinical Dementia Rating (CDR) scores, were investigated using linear mixed models. We found significantly decreased synaptophysin and SV2A densities in the cortex of PD, PDD and DLB cases compared to controls. Specifically, synaptic density was decreased in cortical regions affected at Braak α -synuclein stage 5 in PD (middle temporal gyrus, anterior cingulate and insula), and was additionally decreased in cortical regions affected at Braak α -synuclein stage 4 in PDD and DLB compared to controls (entorhinal cortex, parahippocampal gyrus and fusiform gyrus). Synaptic loss associated with higher NfL immunoreactivity and LB density. Global synaptophysin loss associated with longer disease duration and higher CDR scores. Synaptic neurodegeneration occurred in temporal, cingulate and insular cortices in PD, as well as in parahippocampal regions in PDD and DLB. In addition, synaptic loss was linked to axonal damage and severe α -synuclein burden. These results, together with the association between synaptic loss and disease progression and cognitive impairment, indicate that regional synaptic loss may underlie clinical differences between PD and PDD/DLB. Our results might provide useful information for the interpretation of synaptic biomarkers in vivo.

Keywords SV2A, Synaptophysin, Neurofilament light chain, Amyloid-beta, P-tau

*Correspondence:
Irene Frigerio
i.frigerio@amsterdamumc.nl

Full list of author information is available at the end of the article



© The Author(s) 2023. **Open Access** This article is licensed under a Creative Commons Attribution 4.0 International License, which permits use, sharing, adaptation, distribution and reproduction in any medium or format, as long as you give appropriate credit to the original author(s) and the source, provide a link to the Creative Commons licence, and indicate if changes were made. The images or other third party material in this article are included in the article's Creative Commons licence, unless indicated otherwise in a credit line to the material. If material is not included in the article's Creative Commons licence and your intended use is not permitted by statutory regulation or exceeds the permitted use, you will need to obtain permission directly from the copyright holder. To view a copy of this licence, visit <http://creativecommons.org/licenses/by/4.0/>. The Creative Commons Public Domain Dedication waiver (<http://creativecommons.org/publicdomain/zero/1.0/>) applies to the data made available in this article, unless otherwise stated in a credit line to the data.

Introduction

Synaptic loss is an early phenomena in Parkinson's disease (PD) and Dementia with Lewy bodies (DLB) [1, 2]. PD is the second most common neurodegenerative disorder, affecting almost 3% of the population over 65 years old [3], and 80% of PD patients develop dementia (PDD) after 20 years of disease onset [4–7]. When patients develop dementia before or within one year of motor symptom onset, the disease is diagnosed as DLB [8]. Pathologically, PD(D) and DLB are synucleinopathies [9], with neuropathological hallmarks of Lewy bodies (LBs) and Lewy neurites [10], consisting mainly of the protein α -synuclein, disrupted organelles, membranes and lipids [11]. In physiological conditions, α -synuclein is abundant in the pre-synaptic compartment [12]. Post-mortem and experimental studies provided evidence that α -synuclein aggregation might start at pre-synaptic terminals, inducing synaptic degeneration and subsequently neuronal loss [1, 13, 14]. In post-mortem brains, a loss of synaptophysin [15] and several other synaptic proteins [16] was reported in frontal, occipital and hippocampal regions in PD, and in the parietal cortex in DLB [17]. However, there is still limited knowledge on the regional patterns of synaptic loss in PD, PDD and DLB, as these studies only included a limited number of regions.

Since PD is increasingly recognized as a synaptopathy [13], many efforts have been made to identify fluid biomarkers of synaptic loss [18–21], and imaging positron emission tomography (PET) tracers reflecting synaptic density [22]. The increasing efforts have led to the discovery that in PD and DLB patients, levels of several synaptic proteins are altered in CSF [18–21], and that binding of the PET tracer synaptic vesicle glycoprotein 2 (SV2A) is reduced in the brainstem and cortex [23–25], even though regional results remain inconsistent across studies. Moreover, limited information is available on the neuropathological alterations linked to synaptic loss in PD, PDD and DLB. In fact, besides α -synuclein pathology, Alzheimer's disease (AD) co-pathology [26–28] and axonal degeneration [29, 30] are often present in the cortex of PDD and DLB patients, and might contribute to regional synaptic degeneration in these phenotypes. Taken together, studying regional differences in synaptic degeneration, and which neuropathological processes contribute to it, may provide insights into the selective vulnerability and neuropathological disease progression of PD(D) and DLB cases.

As such, the aim of this study was to map and quantify synaptic loss with the pre-synaptic markers synaptophysin and SV2A in eight cortical brain regions commonly affected in PD(D) and DLB, and to assess whether regional differences in the pattern of synaptic loss are linked to axonal degeneration and neuropathological burden. We hypothesized that cortical brain

regions affected at Braak α -synuclein stage 4, such as the entorhinal cortex, parahippocampal and fusiform gyrus, show more pronounced synaptic loss than regions affected at stages 5 and 6, such as the temporal, cingulate, insular, and frontal cortices. Moreover, we hypothesized that axonal degeneration and neuropathological burden, especially α -synuclein load, correlate with synaptic loss. The results of this study might provide useful information for the interpretation of synaptic biomarkers in vivo.

Materials and methods

Donor inclusion

In collaboration with the Netherlands Brain Bank (NBB; <http://brainbank.nl>) and Normal Aging Brain Collection Amsterdam (NABCA; <http://nabca.eu>) [31] we included a total of 47 brain donors. 12 PD, 9 PDD and 6 DLB were included based on clinical presentation [7, 8, 32]. Age at diagnosis (symptoms onset), disease duration (age at death minus age at diagnosis), motor-to-dementia interval (years between motor symptoms and dementia onset) and Clinical Dementia Rating scores (CDR) [33] were extracted from the donor's clinical files. Neuropathological diagnosis was confirmed by an expert neuropathologist (A.R.) and performed according to the international guidelines of the Brain Net Europe II (BNE) consortium (<https://www.brainbank.nl/about-us/brain-net-europe/>) [34–36]. Additionally, 20 non-neurological controls were included from the NABCA database [31]. All donors signed an informed consent for brain donation and the use of material and clinical information for research purposes. The procedures for brain tissue collection of NBB and NABCA have been approved by the Medical Ethical Committee of Amsterdam UMC, VUmc. For donor characteristics, see Table S1.

Tissue sampling

Workflow of the methods is visualized in Fig. 1. Brain tissue was collected at autopsy, resulting in an average post-mortem delay (interval between death and autopsy) of 8 hours. Eight formalin-fixed paraffin-embedded tissue blocks (4%, four weeks fixation) were obtained from the right hemisphere and processed for immunohistochemistry. Based on Braak α -synuclein staging [10], we defined 3 groups of brain regions: (i) regions affected at Braak α -synuclein stage 4, consisting of the entorhinal cortex (ENTC), parahippocampal gyrus (PHG) and fusiform gyrus (FusG); (ii) regions affected at Braak α -synuclein stage 5, consisting of the anterior cingulate cortex (ACC), anterior insula (AI), and middle temporal gyrus (MTG); (iii) regions affected at Braak α -synuclein stage 6, consisting of the superior frontal gyrus (GFS) and the posterior cingulate cortex (PCC; the parietal cortex was not available).

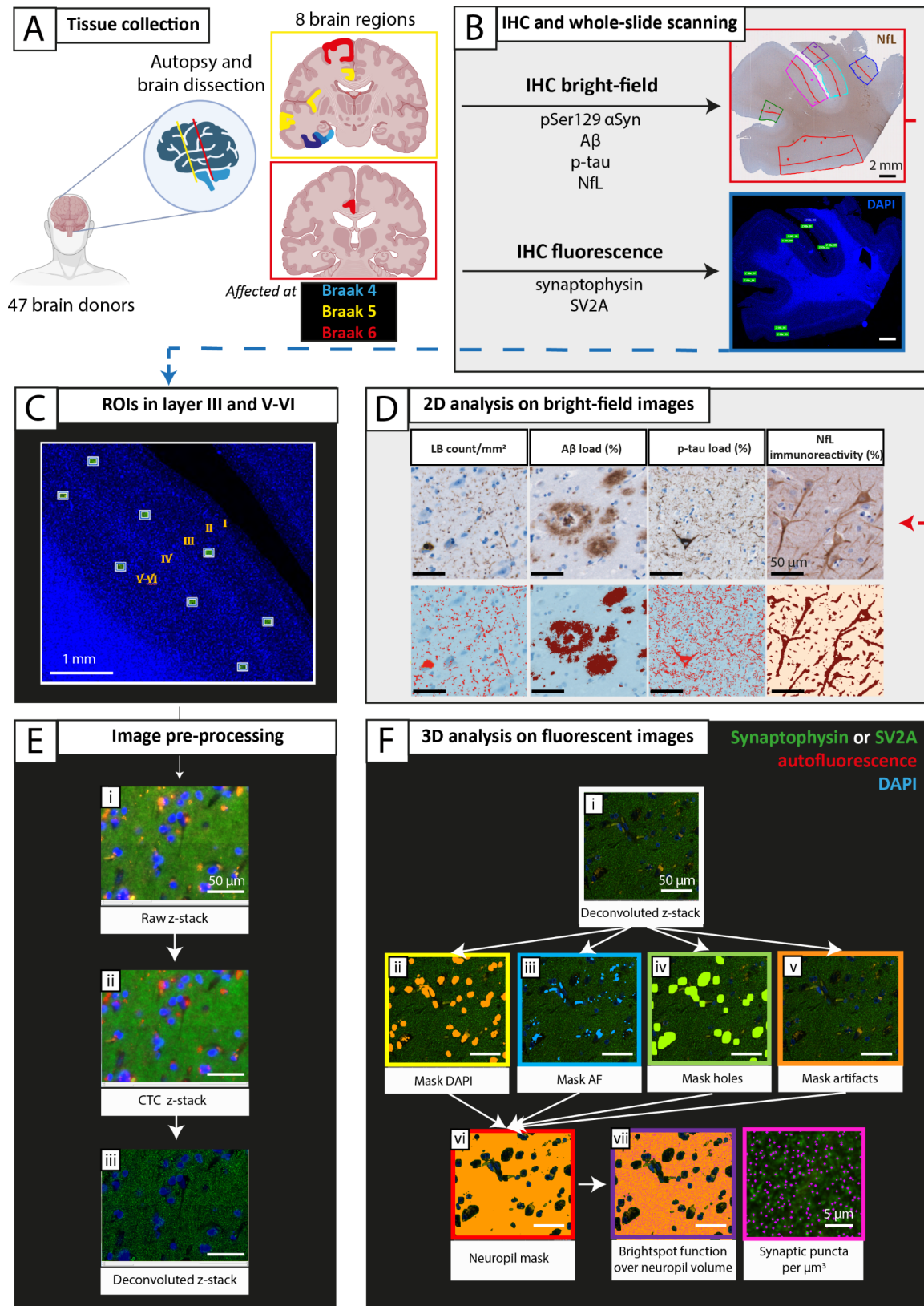


Fig. 1 (See legend on next page.)

(See figure on previous page.)

Fig. 1 Methods workflow. **(A)** After donor inclusion, autopsy was performed, and 8 cortical regions were dissected and grouped into regions affected at [10] Braak α -synuclein stage 4 (in blue), 5 (in yellow), and 6 (in red). **(B)** Brain tissue was processed for immunohistochemistry using antibodies targeting pSer129 α -synuclein, p-tau, A β , and NfL with bright-field, and synaptophysin and SV2A with fluorescence. Whole tissue slides were digitalized, and regions of interest (ROIs) were drawn in superficial (layer I-III) and deep (layer IV-VI) layers of the cortex on bright-field scans, and in the corresponding layer III and layer V-VI on fluorescent scans (detailed ROI placing within cortical minicolumns in **C**) and Fig. S1). **(D)** Subsequently, pixel and object classifiers in QuPath [38] were used to quantify neuropathology load and NfL immunoreactivity on bright-field scans. The ROIs placed on fluorescent scans were **(E)** pre-processed in Huygens Professional, and **(F)** analysed with NIS elements to quantify synaptophysin⁺ and SV2A⁺ puncta per μm^3 in the cortical neuropil volume. For example of artifact removal see Fig. S2. A β : amyloid- β ; AF: autofluorescence; CTC: cross-talk correction; IHC: immunohistochemistry; LB: Lewy body; NfL: neurofilament light chain; pSer129- α Syn: α -synuclein phosphorylated at Ser129; p-tau: phosphorylated tau; ROI: region of interest; SV2A: synaptic vesicle glycoprotein 2 A

Immunohistochemistry

6 μm -thick sections from tissue blocks of the above-mentioned regions were cut and mounted on superfrost+ glass slides (Thermo Scientific, USA). All sections were stained for synaptophysin (C-terminal), SV2A (clone EPR23500-32), pSer129 α -synuclein (clone EP1536Y), amyloid- β (clone 4G8), p-tau (clone AT8) and neurofilament light chain (NfL, amino acid sequence 1-376) (for information on primary antibodies and dilutions see Table S2). Briefly, the sections were deparaffinised, immersed in buffer, and heated to 100°C in a steam cooker for 30 minutes for antigen retrieval. The sections were blocked for endogenous peroxidase using 1% hydrogen peroxide in tris buffered saline (TBS; pH 7.4), and consequently in 3% normal donkey serum in TBS (Triton 0.5%). For the synaptic stainings, Triton was not used to avoid synaptic vesicles to be washed away. Primary antibodies were added, and the sections incubated overnight at 4°C. Primary antibodies were detected using secondary antibodies labelled to Alexa 488, and the sections were counterstained with DAPI and mounted with Mowiol (Sigma-Aldrich, St. Louis, United States) plus anti-fading agent DABCO. For bright-field stainings (pSer129 α -synuclein, amyloid- β , p-tau, and NfL), primary antibodies were diluted in 1% normal donkey serum in TBS (Triton 0.1%) and incubated overnight at 4°C. Primary antibodies were detected using EnVision (Dako, Glostrup, Denmark), and visualized using 3,3'-Diaminobenzidine (DAB, Dako) with Imidazole (50 mg DAB, 350 mg Imidazole and 30 μL of H_2O_2 per 100 mL of Tris-HCl 30 mM, pH 7.6). The sections were counterstained with haematoxylin, after which were dehydrated and mounted with Entellan (Merck, Darmstadt, Germany). In between steps, TBS was used to wash the sections.

Image analysis

Microscopy of synaptic staining

Synaptic imaging was performed using Olympus VS200 (Evident). First, an overview fluorescence scan was performed using a 10x objective (NA 0.40) on the DAPI channel (Fig. 1B). Once the overview scans were obtained, 10 regions of interest (ROIs) (200 \times 160 μm) were placed within the cortex. Specifically, 5 ROIs were

placed in cortical layer III, and 5 ROIs in cortical layers V-VI. Each pair of ROIs (one in cortical layer III, and one in cortical layer V-VI) was placed within a cortical minicolumn (Fig. 1C, for details see Fig. S1), corresponding to the superficial and deep pyramidal layers of the cortex, commonly affected in PD(D) and DLB [10, 15]. To ensure correspondence between ROIs for pathological/neurofilament and synaptic measurements, fluorescence ROIs were placed within the corresponding bright-field ROIs of adjacent sections (Fig. 1B, for details see Fig. S3). Slides were scanned overnight with 60x oil objective (NA 1.42) on 3 channels: DAPI, Alexa 488 (targeting synaptophysin or SV2A) and autofluorescence (see Table S3 for scanning details). Images were taken as z-stacks to allow deconvolution and 3D image analysis. Specifically, 2 images were acquired above and 2 under the focus point, with a step size of 0.28 μm in the z-direction. The scans were visually inspected for artifacts, and if needed, re-scans were immediately performed.

Image processing and 3D analysis of synaptic markers

Image pre-processing was performed with Huygens Professional (<https://svi.nl/Huygens-Professional>). First, cross-talk correction (CTC) was performed for subtraction of the autofluorescence signal (such as blood vessels, lipofuscin and artifacts, Fig. 1E, ii), and next color deconvolution was performed (Fig. 1E, iii). Subsequently, NIS-elements AR analysis version 5.42.00 (<https://www.microscope.healthcare.nikon.com/products/software/nis-elements>) was used to quantify synaptic density over volume (Fig. 1F). Images were masked to define the neuropil volume by applying and inverting masks for (1) nuclei on the DAPI channel (Fig. 1E, ii), (2) blood vessels on the autofluorescence channel (Fig. 1E, iii), (3) holes in the tissue on the Alexa 488 channel (Fig. 1E, iv), (4) and tissue artifacts such as foldings and bubbles on the Alexa 488 channel (Fig. 1E, v; for an example of artifact removal see Fig. S2). Finally, all masks were inverted and combined (Fig. 1E, vi) to define the neuropil volume in which synaptic puncta were counted. As synaptic diameter varies approximately between 0.1 and 1 μm [37], we incrementally inputted a diameter from 0.1 to 1 μm to identify the synaptic puncta. 0.6 μm and 0.5 μm were the diameters that recognized all synaptophysin-positive

(synaptophysin+) and SV2A-positive (SV2A+) puncta, respectively. Synaptic puncta were finally counted with the 'bright spots' function, based on diameter and intensity (Fig. 1F, vii). The outcome measures were number of synaptophysin⁺ and SV2A⁺ puncta/ μm^3 per ROI, yielding a total of ~3700 data points for each synaptic marker across all cases and regions. Extreme outliers (which lie more than 3 times the interquartile range) were quality checked and excluded if necessary.

Quantification of NfL and pathological hallmarks

Using a whole-slide scanner (Vectra Polaris, 20x objective) images of NfL, pSer129 α -synuclein, amyloid- β and p-tau immunostained sections were taken and quantified using QuPath 0.2.3 stardist (<https://qupath.readthedocs.io/en/0.2/>) [38]. ROIs containing all cortical layers were delineated in straight areas of the cortex to avoid over- or underestimation of pathology in sulci and gyri, respectively [39], as described before [29, 40]. The cortex was further segmented into superficial (I-III) and deep (IV-VI) cortical layers based on the haematoxylin counterstaining. The entorhinal cortex, parahippocampal gyrus and fusiform gyrus were segmented as described before [29] (for details, see Fig. S3). Amyloid- β and p-tau stainings of control cases were delineated in superficial (layer I-III) and deep cortical layers (layer IV-VI) only in entorhinal, parahippocampal and fusiform gyrus. DAB immunoreactivity was quantified with in-house QuPath scripts, using pixel and object classifiers, as done previously [29]. The outcome measures for NfL was %area load, expressed in the text as %immunoreactivity. The outcome measure for pSer129 α -synuclein was LB density (LB count/ mm^2), while outcome measures for amyloid- β and p-tau were %area load (Fig. 1D).

Statistics

Statistical analyses were performed in SPSS 28.0 (Chicago, IL). Normality was tested, and demographics between PD, PDD, DLB and control groups were compared using one-way ANOVA or Kruskal-Wallis test for continuous data, and Fisher exact test for categorical data. Since the data have a nested design (8 brain regions per donors, 10 ROIs per brain region in 2 cortical layers) multi-level linear mixed models (LMM) were used to compare synaptic densities between groups, with case ID, brain area and cortical layer as nested variables, and with age and sex as covariates. In order to associate synaptic density with regional neuropathological load, we averaged the 5 measurements in cortical layer III and V-VI to have one measure for superficial and deep cortical layers, respectively, corresponding to the data format of neuropathological load, and therefore corresponding the synaptic and neuropathological data within the same ROIs. A logarithmic transformation (\log_{10}) was

applied to measures of LB density, amyloid-beta load and p-tau load after adding a constant (+1) to avoid zeros to become undefined values. To assess associations across all regions between synaptic density and neuropathology load or NfL immunoreactivity, synaptic density was the dependent variable and neuropathology load or neurofilament immunoreactivity (independent variable) were the main effects, together with age and sex (i.e. covariates). The intercept was included in all analyses as random effect. Multiple pairwise (post-hoc) comparison corrections were performed using Bonferroni post-hoc test, and multiple testing comparison corrections were performed with Bonferroni method, after which p -values < 0.05 were considered significant. Group comparisons were expressed as percentage differences, as in the formula: %difference = [(absolute difference)/mean control]*100. Correlation coefficients (r) of LMM associations were calculated as in the formula: $r = (\text{estimate fixed effect} * \text{standard deviation fixed effect}) / \text{standard deviation dependent variable}$. Finally, we predicted synaptic density by adding all variables in the model (age, sex, neuropathological load and NfL immunoreactivity), always including the intercept as random effect.

Results

Cohort description

Clinical and neuropathological data of included PD, PDD, DLB and non-neurological control donors are summarized in Table 1 (and per donor in Table S1). Sex, age at diagnosis, and post-mortem delay did not differ between groups. PD donors were significantly older at death than controls (mean 82 vs. 72 years, $p=0.016$). Disease duration was significantly shorter for DLB compared to PD donors (mean 5 vs. 18 years, $p<0.001$) and PDD (mean 5 vs. 14 years, $p=0.012$). CDR scores were significantly higher in PDD ($p=0.024$) and DLB ($p=0.006$) compared to PD donors. Pathologically, DLB donors showed significantly more AD co-pathology compared to controls (ABC score: $p<0.002$, Thal phase: $p=0.010$, Braak NFT stage: $p<0.001$), but not compared to PD and PDD cases ($p>0.05$). Moreover, DLB cases had significantly more cerebral amyloid angiopathy (CAA) type 1 compared to the other groups (DLB: 50% of cases had CAA type 1; controls: 5%, PD: 0%, and PDD: 11%, $p=0.004$). Compared to controls, Braak NFT stage was also significantly higher in PD ($p=0.007$) and PDD ($p=0.048$). For representative images of all outcome measures see Fig. 2, and for quantitative regional cortical neuropathology burden and NfL immunoreactivity see Fig. S4.

Regional synaptophysin and SV2A loss in PD, PDD and DLB

Synaptophysin density was decreased by 4% in PD ($p=0.048$), 7% in PDD ($p<0.001$), and 8% in DLB ($p<0.001$) compared to controls across all regions

	Control	PD	PDD	DLB
N	20	12	9	6
Sex F/M (%F)	11/9 (55%)	3/9 (25%)	5/4 (56%)	1/5 (17%)
Age at diagnosis years, mean [range]	-	64 [54-76]	63 [44-84]	73 [62-88]
Disease duration years, mean [range]	-	18 [13-23]	14 [8-21]	5 ^{††† #} [3-7]
MDI years, mean [range]	-	-	10 [2-16]	0 ^{††} [0-0]
CDR median (N) [range]	n.a.	0.5 (N=5) [0.5-0.5]	2 [†] (N=6) [1-3]	2 ^{††} (N=5) [1-3]
Age at death years, mean [range]	72 [57-87]	82 * [69-93]	77 [62-94]	76 [61-91]
Post-mortem delay hrs:min, mean [range]	8:38 [4:35-12:40]	7:31 [3:00 -10:40]	7:53 [5:10-10:40]	7:21 [4:30-10:10]
Pathological characteristics				
	Control	PD	PDD	DLB
Braak α-synuclein stage [10]	20	12	9	6
N 0/1/2/3/4/5/6	17/2/1/0/0/0/0	0/0/0/0/1/1/1	0/0/0/0/0/0/9	0/0/0/0/0/0/6
ABC score [41] N	20	12	9	6
A 0/1/2/3	4/14/2/0	1/8/3/0	0/4/3/2*	0/1/2/3 **
B 0/1/2/3	4/15/1/0	0/8/3/0	0/6/3/0	0/1/4/1 **
C 0/1/2/3	20/0/0/0	11/1/0/0	6/1/2/0	1/0/4/1 *** †††
Thal phase [42] N	20	12	9	6 **
0/1/2/3/4/5	4/9/5/1/4/0	1/5/3/3/0/0	0/3/1/3/2/0	0/1/0/2/1/2
Braak NFT stage [43] N	20	12 **	9 *	6 ***
0/1/2/3/4/5/6	4/11/4/1/0/0/0	0/3/5/3/1/0/0	0/2/4/1/2/0/0	0/0/1/1/3/0/1
CAA type [44] N	20	12	9	6 [†]
No CAA/type 1/ type 2	16/1/3	11/0/1	6/1/2	2/3**/1

Table 1 Demographic, clinical and pathological characteristics of brain donors. Data are mean, and minimum to maximum range. Legend: CAA: cerebral amyloid angiopathy; CDR: Clinical Dementia Rating; DLB: dementia with Lewy bodies; F: females; hrs: hours; LB: Lewy body; M: males; MDI: motor-to-dementia interval; min: minutes; n.a.: not available; NFT: neurofibrillary tangles; PD: Parkinson's disease; PDD: Parkinson's disease dementia. * $p < 0.05$, ** $p < 0.01$, *** $p < 0.001$ when compared to controls; † $p < 0.05$, †† $p < 0.01$, ††† $p < 0.001$ when compared to PD; # $p < 0.05$, ## $p < 0.01$, ### $p < 0.001$ when compared to PDD

(Fig. 3A). When looking at regions affected at different Braak α -synuclein stages, synaptophysin density was significantly lower in regions affected at Braak 4 (i.e. entorhinal cortex, parahippocampal gyrus and fusiform gyrus combined) in DLB compared to controls (-9%, $p = 0.011$). Additionally, synaptophysin density was significantly lower in regions affected at Braak 5 (i.e. middle temporal gyrus, anterior cingulate cortex and anterior insula combined) in PDD versus controls (-11%, $p < 0.001$) and versus PD (-7%, $p = 0.022$) (Fig. 3C, E). Synaptophysin

density did not differ between groups in regions affected at Braak 6 (i.e. superior frontal gyrus and posterior cingulate cortex combined). In summary, synaptophysin density was decreased in all groups compared to controls, and more specifically in regions affected at Braak 4 in DLB, and in regions affected at Braak 5 in PDD.

SV2A density was decreased by 5% in PD ($p = 0.006$), and 6% in PDD ($p < 0.001$), and did not differ in DLB ($p = 0.105$) compared to controls across all regions (Fig. 3B). When looking at regions affected at different

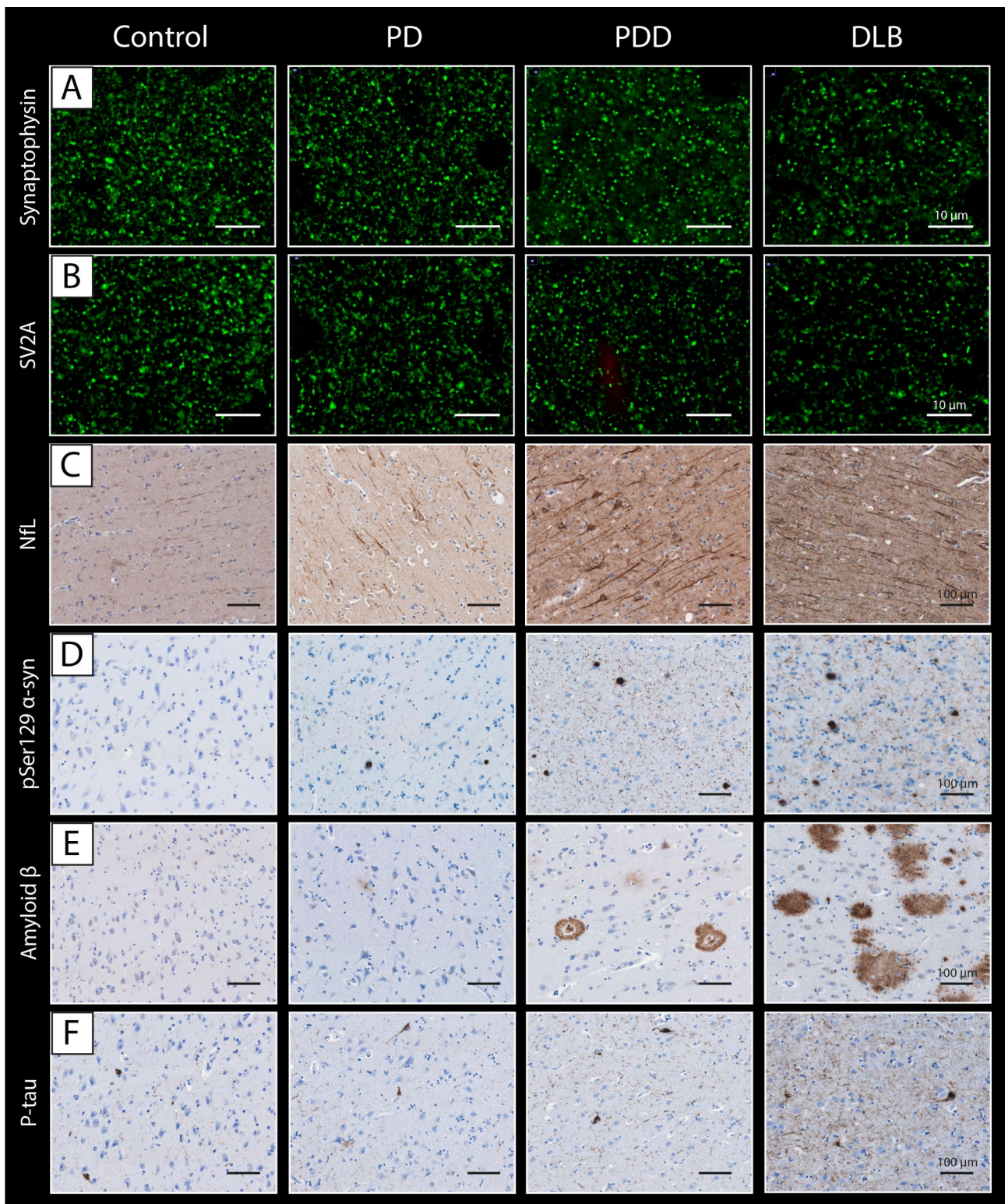
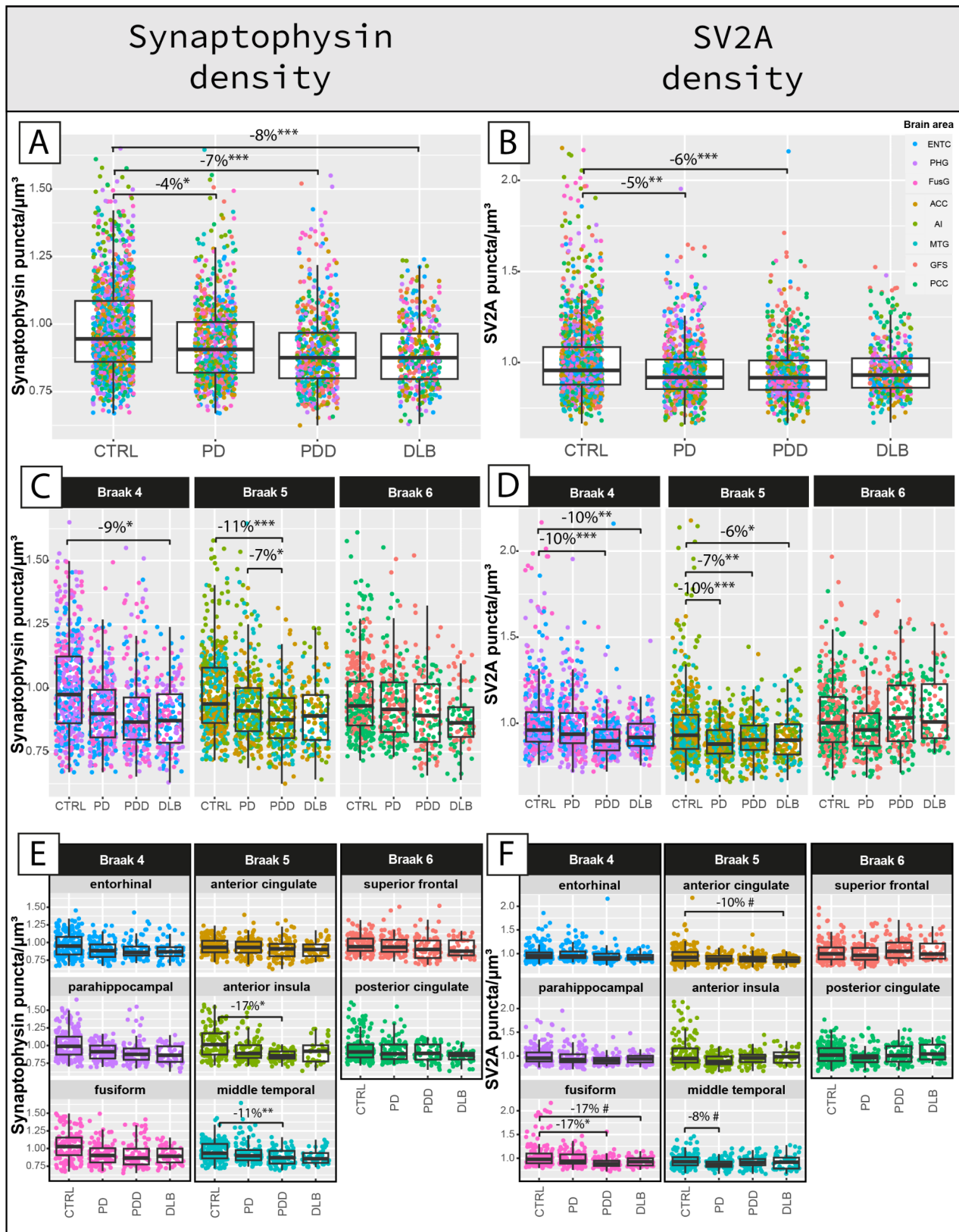


Fig. 2 Representative images of synaptic puncta, NFL and pathological hallmarks in controls, PD, PDD, and DLB donors. Representative images of (A) synaptophysin⁺ pre-synaptic puncta, (B) SV2A⁺ pre-synaptic puncta, (C) NFL, (D) pSer129 α-synuclein, (E) amyloid-beta and (F) p-tau were acquired in the parahippocampal gyrus of controls, PD, PDD and DLB donors. **Legend:** DLB: Dementia with Lewy Bodies; NFL: neurofilament light chain; PD: Parkinson's disease; PDD: Parkinson's disease dementia; p-tau: phosphorylated tau



(See figure on previous page.)

Fig. 3 Synaptophysin and SV2A density are reduced in PD, PDD and DLB in a region-specific manner compared to controls. **A,B**) The first row shows the group differences in synaptophysin and SV2A density across all cases, **C,D**) the second row shows the same group differences within regions grouped per brain areas affected at Braak 4, 5 and 6, and **E, F**) the last row shows the same group differences within brain areas. Every data point represents one measurement color-coded by brain area. Linear mixed model p-values are adjusted for multiple pairwise (post-hoc) comparisons between groups and multiple testing comparisons for regions affected at Braak stage 4, 5, and 6 in **C**) and **D**), and for 8 regions in **E**) and **F**). # $p < 0.100$, * $p < 0.05$, ** $p < 0.01$, *** $p < 0.001$ after Bonferroni post-hoc test. ACC: anterior cingulate cortex; AI: anterior insula; CTRL: control; DLB: Dementia with Lewy bodies; ENT: entorhinal cortex; FusG: fusiform gyrus; GFS: superior frontal gyrus; MTG: middle temporal gyrus; PCC: posterior cingulate cortex; PD: Parkinson's disease; PDD: Parkinson's disease dementia; PHG: parahippocampal gyrus. # $p < 0.10$, * $p < 0.05$, ** $p < 0.01$, *** $p < 0.001$

Braak α -synuclein stages, SV2A density was significantly lower in regions affected at Braak 4 in DLB (-10%, $p = 0.001$) and PDD (-10%, $p < 0.001$) compared to controls, and in regions affected at Braak 5 in PD (-10%, $p < 0.001$), PDD (-7%, $p = 0.003$) and DLB (-6%, $p = 0.047$) compared to controls (Fig. 3D, F). SV2A density did not differ between groups in regions affected at Braak 6. In summary, SV2A density was decreased in all groups compared to controls, specifically in regions affected at Braak 4 in DLB and PDD (especially the fusiform gyrus), and in regions affected at Braak 5 in all groups.

Synaptic density decreased with age and was higher in females (supplementary results and Fig. S5), and was slightly higher in layer III compared to layer V-VI (supplementary results and Fig. S6). Layer III and V-VI seemed to be similarly affected in PD, PDD, DLB (Fig. S7). Within-groups, synaptophysin density was similar across brain regions, while SV2A density was significantly higher in regions affected at Braak stage 6 in PD, PDD and DLB (supplementary results and Fig. S8). As such, regional synaptophysin and SV2A density only weakly correlated (supplementary results and Fig. S9).

Cortical synaptic loss is associated with NfL immunoreactivity

We previously showed that NfL accumulates in cortical brain regions in PDD and DLB compared to controls, and that increased NfL immunoreactivity can be considered a proxy of axonal fragmentation and degeneration [29]. Here, we investigated whether cortical synaptic density correlated with regional NfL immunoreactivity.

Both synaptophysin ($r = -0.16$, $p < 0.001$) and SV2A density ($r = -0.08$, $p = 0.033$) negatively correlated with NfL immunoreactivity across all cases. Regionally (Fig. 4A), synaptophysin density showed a strong negative correlation with NfL immunoreactivity specifically in the regions affected at Braak 6 in DLB cases ($r = -0.68$, $R^2 = 46\%$, $p = 0.048$), and not in any region of any other groups ($p > 0.05$). Regarding SV2A density (Fig. 4B), a significant negative correlation with NfL immunoreactivity was found in the regions affected at Braak 4 of PD cases ($r = -0.35$, $R^2 = 12\%$, $p = 0.030$), and at Braak 6 of DLB cases ($r = -0.83$, $R^2 = 69\%$, $p < 0.001$).

Taken together, cortical synaptic density associated with increased NfL immunoreactivity in PD and DLB. Particularly, regions affected at Braak 6 of DLB cases

showed the strongest correlation, where NfL immunoreactivity accounted for up to 70% of the variability in SV2A density.

Synaptic loss is more severe in cortical brain regions with higher LB density

Synaptophysin density (PD+PDD+DLB: $r = -0.12$, $R^2 = 1\%$, $p = 0.006$) and SV2A (PD+PDD+DLB: $r = -0.18$, $R^2 = 3\%$, $p < 0.001$), negatively correlated with LB density across all regions in the disease groups. Regionally (Fig. 5A), synaptophysin density negatively correlated with LB density in regions affected at Braak 4 in PD ($r = -0.46$, $R^2 = 21\%$, $p = 0.011$) and DLB groups ($r = -0.48$, $R^2 = 23\%$, $p = 0.005$), and in regions affected at Braak 6 in PDD ($r = -0.55$, $R^2 = 30\%$, $p = 0.039$). Synaptophysin density did not correlate with LB density in any other region ($p > 0.05$). Moreover, SV2A density correlated negatively with LB density in regions affected at Braak 4 in PD ($r = -0.39$, $R^2 = 15\%$, $p = 0.022$), but not in other regions or groups (Fig. 5B).

Taken together, increased LB density associated with synaptophysin and SV2A loss mostly in regions affected at Braak 4, which are the regions showing the highest LB density (Fig. S4).

Higher SV2A density is linked to higher amyloid- β load

SV2A density, but not synaptophysin ($p = 0.453$), positively correlated with amyloid- β load across all regions of all cases ($r = 0.14$, $R^2 = 2\%$, $p = 0.001$). Regionally, synaptophysin density negatively correlated with amyloid- β load in regions affected at Braak 4 of DLB cases ($r = -0.52$, $R^2 = 27\%$, $p = 0.023$) (Fig. 6A). As a strong negative association was found in these regions with LB pathology (see previous paragraph), we corrected for LB density in the analysis. Indeed, decreased synaptophysin density in regions affected at Braak 4 tended to be driven by LB density rather than amyloid- β load (amyloid- β : $p = 0.305$; LB density: $p = 0.055$). SV2A density positively correlated with amyloid- β load in regions affected at Braak 6 in DLB ($r = 0.76$, $R^2 = 58\%$, $p < 0.001$), but not in other groups ($p > 0.05$) (Fig. 6B).

Taken together, higher SV2A density in DLB was associated with higher amyloid- β load in regions affected at Braak 6, where amyloid- β load accounted for almost 60% of the variability in SV2A density. No effects for synaptophysin were found after correcting for LB pathology.

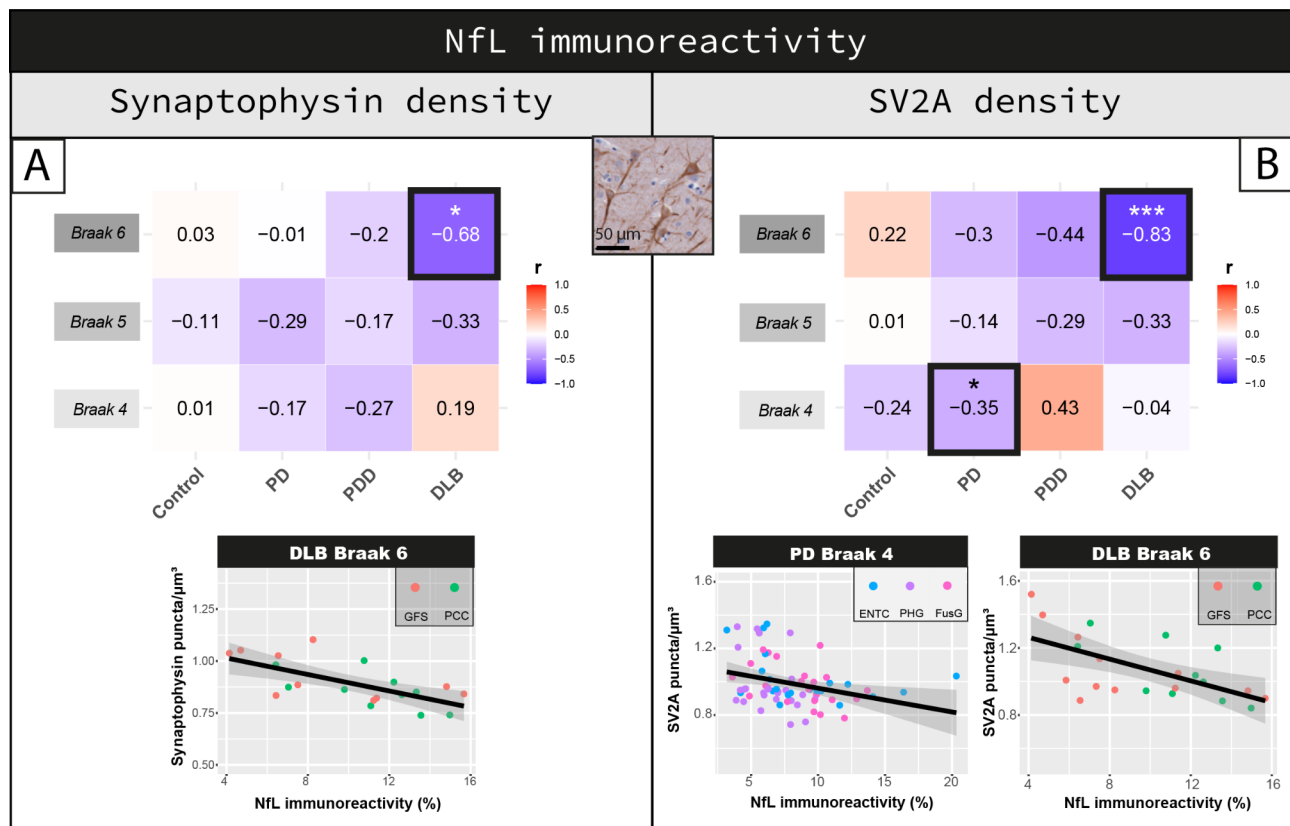


Fig. 4 Inverse correlation between synaptophysin or SV2A and NfL density. Correlation of NfL immunoreactivity with **(A)** synaptophysin and **(B)** SV2A density are shown per group in regions affected at Braak 4, 5 and 6. Heat-maps are color-coded for correlation coefficient (r), being blues representative of negative correlations and reds of positive correlations. For each correlation, the correlation coefficient is reported, together with its p-value. For the correlations highlighted with a square we are also reporting the scatterplots, color-coded for brain area (every data point represents one averaged measurement per layer III and V-VI). Linear mixed model p-values are adjusted for multiple testing (12 correlations per synaptic marker) * $p < 0.05$, ** $p < 0.01$, *** $p < 0.001$ after Bonferroni method. **Legend:** DLB: Dementia with Lewy bodies; ENTc: entorhinal cortex; FusG: fusiform gyrus; GFS: superior frontal gyrus; NfL: neurofilament light chain; PCC: posterior cingulate cortex; PD: Parkinson's disease; PDD: Parkinson's disease dementia; PHG: parahippocampal gyrus

P-tau load has differential effects on synaptophysin and SV2A density

Synaptophysin density, and not SV2A ($p = 0.598$), negatively correlated with p-tau load across all regions of all cases ($r = -0.10$, $R^2 = 1\%$, $p = 0.022$). Regionally, synaptophysin density did not correlate with p-tau load in any region of any group ($p > 0.05$) (Fig. 7A). SV2A density positively correlated with p-tau load in regions affected at Braak 4 in PDD ($r = 0.85$, $R^2 = 72\%$, $p < 0.001$), but not in other groups (> 0.05) (Fig. 7B). As a similar association was found in this region for amyloid- β load (see Fig. 6), we assessed if this association was driven by amyloid- β . Increased SV2A density in regions affected at Braak 4 in PDD cases was driven by an increase in amyloid- β load rather than p-tau load (amyloid- β : $r = 1.00$, $p < 0.001$; p-tau: $r = -0.74$, $p = 0.044$).

Taken together, p-tau load seemed to have differential effects on synaptophysin and SV2A density. P-tau weakly correlated with synaptophysin density across all regions, while it positively associated with SV2A density

in regions affected at Braak 4 in PDD, but this effect was mostly driven by amyloid- β load.

Synaptic degeneration is linked to axonal damage, higher LB density and older age

We investigated the combined contribution of age, sex, NfL immunoreactivity, LB density, amyloid- β and p-tau load on synaptophysin and SV2A density by including all these markers in the same model (for models in regions affected at Braak stage 4, 5 and 6 see Table S4).

For synaptophysin, the model explained 56% of the variance (R^2) when including all cases. The strongest negative associations were observed between synaptophysin density and LB density ($\beta = -0.074$, $p < 0.001$), NfL immunoreactivity ($\beta = -0.008$, $p = 0.001$), and age ($\beta = -0.002$, $p = 0.017$). When looking at the model including only the diseased groups (PD+PDD+DLB) ($R^2 = 54\%$), LB density ($\beta = -0.053$, $p = 0.019$), and NfL immunoreactivity ($\beta = -0.008$, $p < 0.001$) were the negative predictors of synaptophysin density.

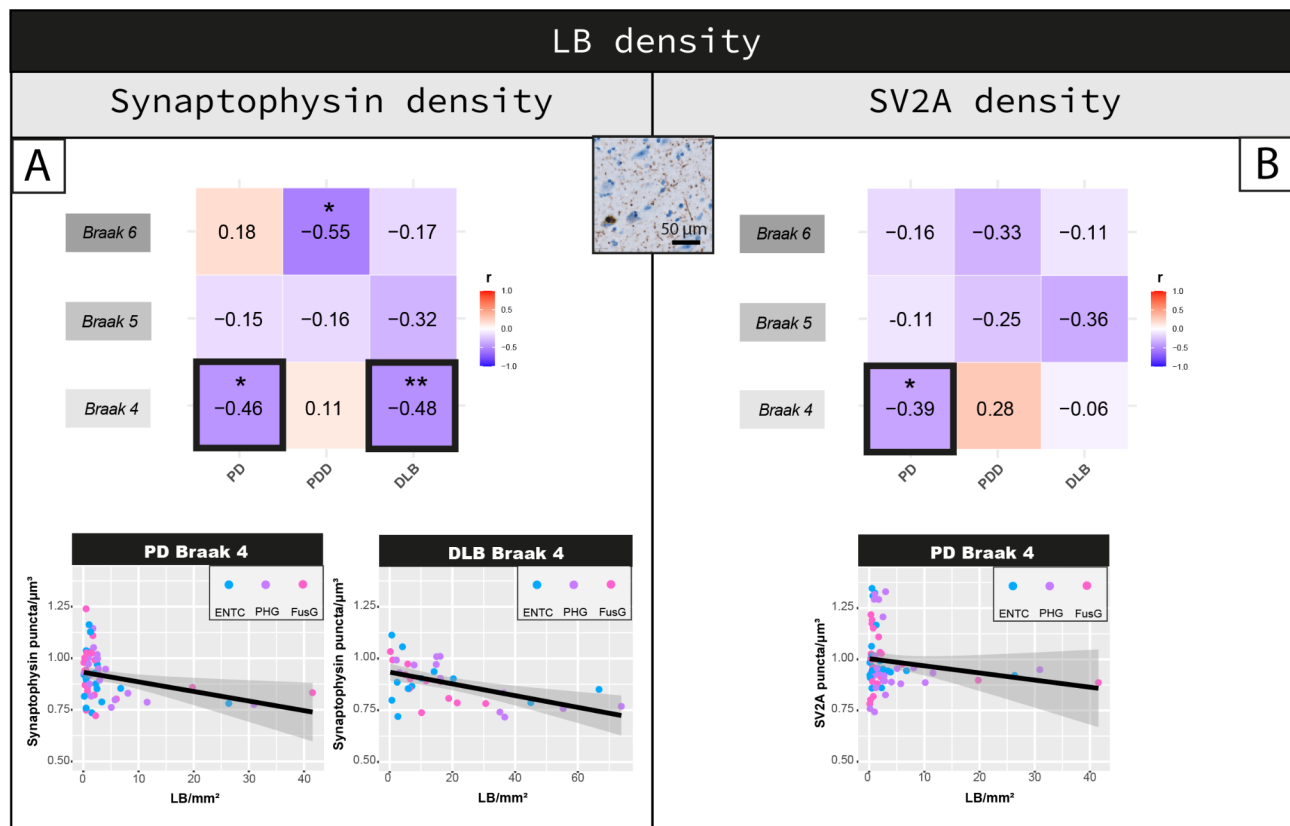


Fig. 5 Cortical synaptophysin and SV2A density shows an inverse correlation with LB density in regions affected at Braak stage 4 in PD and DLB. Correlation between LB density and **(A)** synaptophysin and **(B)** SV2A density are shown per groups per regions affected at Braak 4, 5 and 6. Heat-maps are color-coded for correlation coefficient (r), being blues representative of negative correlations and reds of positive correlations. For each correlation, the correlation coefficient is reported, together with its p -value. Linear mixed model p -values are adjusted for multiple testing (9 correlations per synaptic marker). * $p < 0.05$, ** $p < 0.01$, *** $p < 0.001$ after Bonferroni method. For the correlations highlighted with a square we are also reporting the scatterplots, color-coded for brain area (every data point represents one averaged measurement per layer III and V-VI). **Legend:** DLB: Dementia with Lewy bodies; ENTG: entorhinal cortex; FusG: fusiform gyrus; LB: Lewy body; PD: Parkinson's disease; PDD: Parkinson's disease dementia; PHG: parahippocampal gyrus

For SV2A, an explained variance of 57% was observed across all cases. The strongest negative associations were seen between SV2A density and LB density ($\beta = -0.103$, $p < 0.001$), NfL immunoreactivity ($\beta = -0.007$, $p = 0.002$), and age ($\beta = -0.002$, $p = 0.021$), and a positive association for amyloid- β load ($\beta = 0.170$, $p < 0.001$). When looking at the model including only the diseased groups (PD+PDD+DLB) ($R^2 = 61\%$), the results did not change: the negative predictors were again LB density ($\beta = -0.130$, $p < 0.001$), NfL immunoreactivity ($\beta = -0.006$, $p = 0.003$), and age ($\beta = -0.004$, $p < 0.001$), and the only positive predictor amyloid- β load ($\beta = 0.210$, $p < 0.001$).

Taken together, both synaptophysin and SV2A loss associated with increased LB density, NfL immunoreactivity, and age. Amyloid- β load was a specific positive predictor for SV2A density. Both models explained 56 to 61% of the variance in synaptic density.

Cortical synaptophysin loss is more severe in cases with lower cognitive scores

Lastly, we investigated whether cortical synaptophysin and SV2A density correlated with clinical measures, including disease duration, motor-to-dementia interval and CDR scores.

Longer disease duration significantly correlated with cortical synaptophysin loss in DLB cases ($r = -0.27$, $p = 0.009$) and with cortical SV2A loss in PDD cases ($r = -0.19$, $p = 0.015$). A longer motor-to-dementia interval correlated with cortical SV2A loss in PDD cases ($r = -0.32$, $p < 0.001$), but not with cortical synaptophysin loss ($p > 0.05$). Higher CDR scores significantly associated with cortical synaptophysin loss ($r = -0.21$, $p < 0.001$), but not with SV2A loss ($p = 0.179$).

Taken together, we found that longer disease duration, longer motor-to-dementia interval and higher CDR scores correlated with cortical synaptic loss.

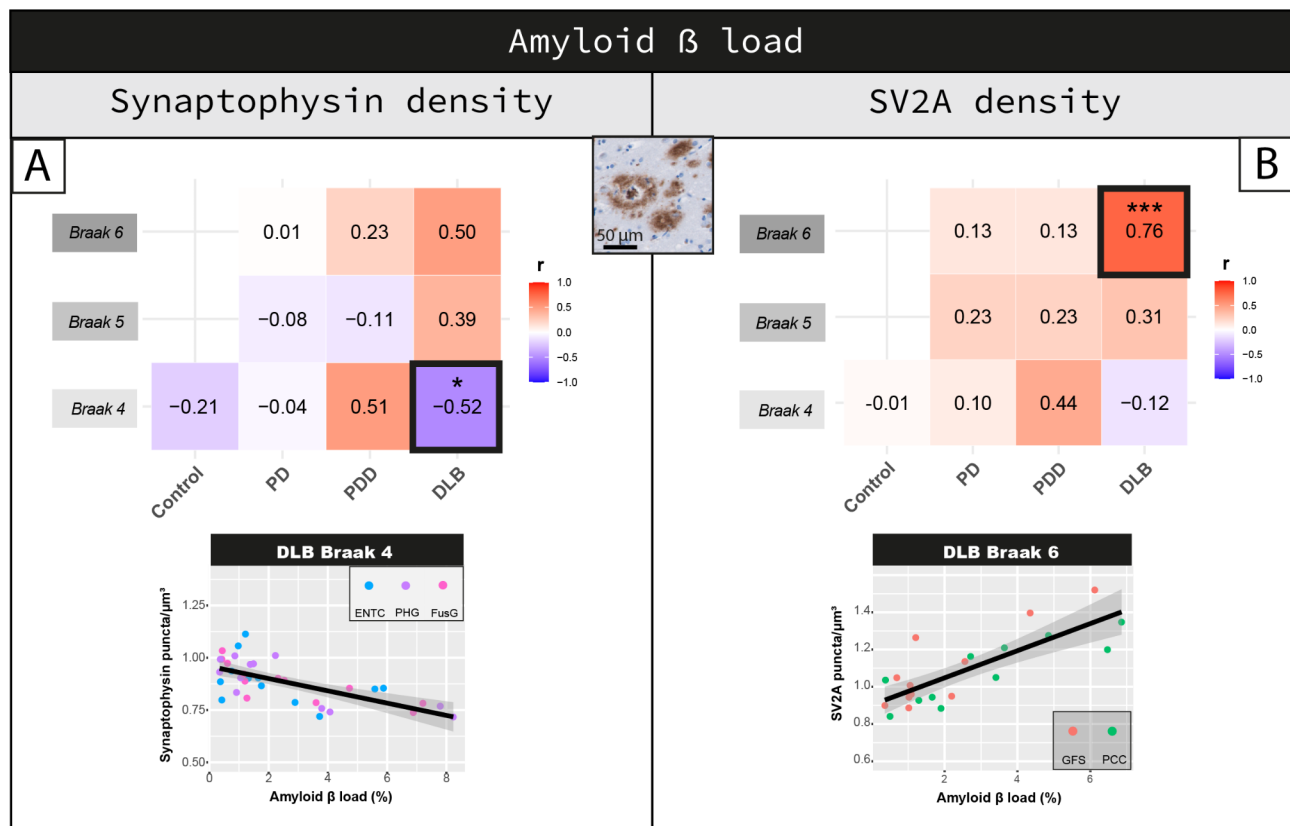


Fig. 6 Cortical SV2A density shows a positive correlation with amyloid- β load in DLB. Correlation between amyloid- β load and (A) synaptophysin and (B) SV2A density are shown per group in regions affected at Braak 4, 5 and 6. Heat-maps are color-coded for correlation coefficient (r), being blues representative of negative correlations and reds of positive correlations. For each correlation, the correlation coefficient is reported, together with its p -value. Linear mixed model p -values are adjusted for multiple testing (10 correlations per synaptic marker). # $p < 0.100$, * $p < 0.05$, *** $p < 0.001$, **** $p < 0.0001$ after Bonferroni method. For the correlations highlighted with a square we are also reporting the scatterplots, color-coded for brain area (every data point represents one averaged measurement per layer III and V-VI). **Legend:** DLB: Dementia with Lewy bodies; ENTc: entorhinal cortex; FusG: fusiform gyrus; GFS: superior frontal gyrus; PCC: posterior cingulate cortex; PD: Parkinson's disease; PDD: Parkinson's disease dementia; PHG: parahippocampal gyrus

Discussion

Using a high throughput immunofluorescence approach, we mapped and quantified synaptic loss in eight cortical brain regions commonly affected in PD(D) and DLB, and assessed whether regional differences in the pattern of synaptic loss are linked to axonal degeneration and neuropathological burden. We found that synaptic loss was most severe in temporal, cingulate and insular cortices affected at Braak α -synuclein stage 5 in PD, and additionally in parahippocampal regions affected at Braak α -synuclein stage 4 in PDD and DLB, and that synaptic loss associated with NfL immunoreactivity and LB density. Lastly, we found that cortical synaptic degeneration associated with longer disease duration and worse cognitive scores.

Both synaptophysin and SV2A density were decreased in PD, PDD and DLB compared to non-demented controls. The effect size of synaptic loss we found matches well with the literature in both post-mortem and PET studies [15, 24]. Similar to our results of a 4–8% decrease in cortical synaptic density, a post-mortem study found a global reduction of cortical synaptophysin density of 5% in PD and 8% in PDD

compared to age-matched controls [15]. PET studies using a SV2A tracer also reported 3–10% decrease in binding in cortical regions of PD patients [23, 25], which was more pronounced in PDD/DLB [24]. Regionally, we found that cortical regions affected at Braak α -synuclein stage 4 and 5 were more severely affected by synaptic degeneration, while cortical regions affected at Braak α -synuclein stage 6 showed synaptic density comparable to controls. These results suggest that synaptic degeneration occurs in regions affected by α -synuclein, and since Braak α -synuclein stage also describes an increase in α -synuclein load with disease progression, it is probably dependent on the amount of α -synuclein pathology [10]. Furthermore, we found that the pattern of synaptic degeneration differed between PD and PDD/DLB cases: in PD temporal, cingulate and insular cortices affected at Braak α -synuclein stage 5 showed more pronounced synaptic degeneration compared to controls, while PDD and DLB cases additionally showed synaptic degeneration in parahippocampal regions affected at Braak α -synuclein stage 4. These results suggest that the pattern of regional synaptic neurodegeneration differs in PD and

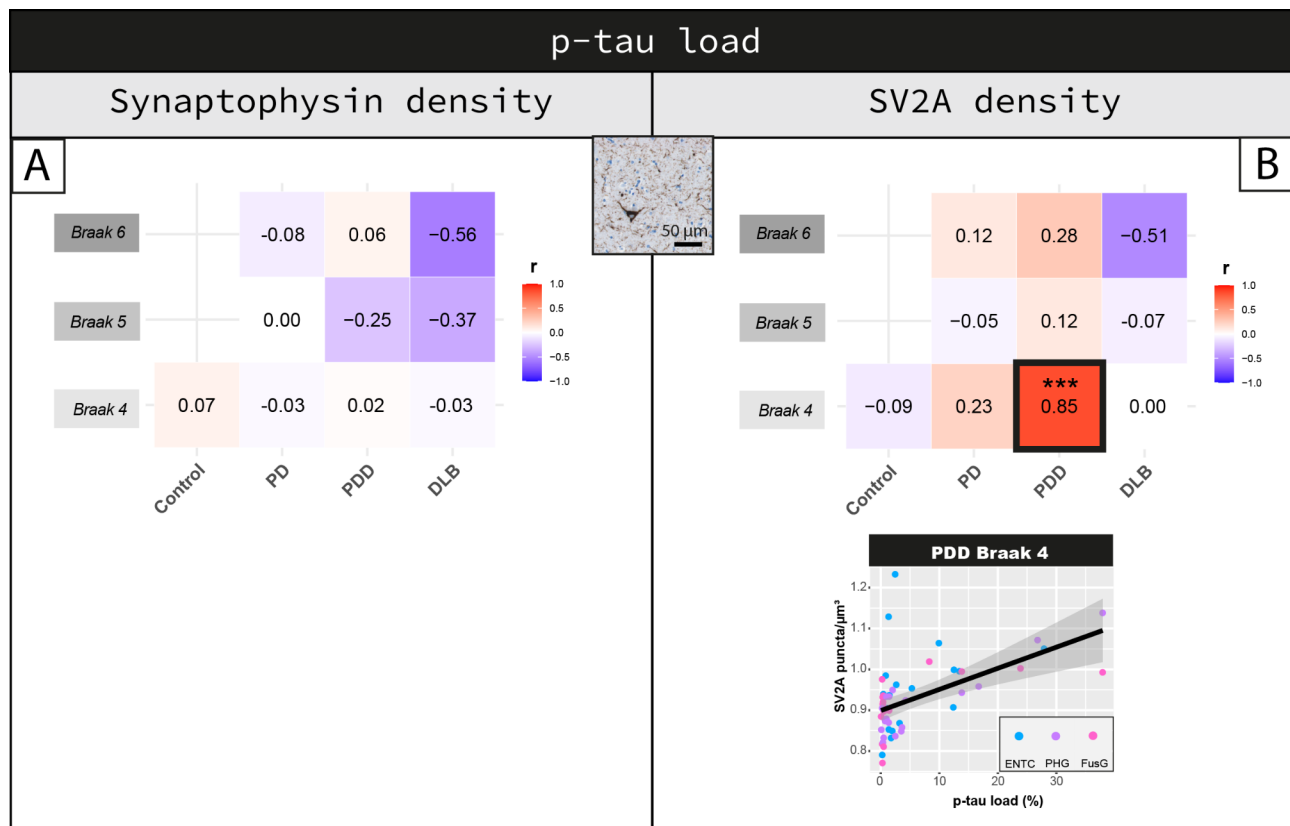


Fig. 7 Cortical synaptophysin and SV2A density differentially correlate with p-tau load. Correlation between p-tau load and **(A)** synaptophysin and **(B)** SV2A density are shown per group in regions affected at Braak 4, 5 and 6. Heat-maps are color-coded for correlation coefficient (r), towards blue represents a negative correlations and towards red a positive correlations. For each correlation, the correlation coefficient is reported, together with its p-value. For the correlations highlighted with a square we are also reporting the scatterplots, color-coded for brain area (every data point represents one averaged measurement per layer III and V-VI). Linear mixed model p-values are adjusted for multiple testing (10 correlations per synaptic marker). * $p < 0.05$, ** $p < 0.01$, *** $p < 0.001$ after Bonferroni method. **Legend:** DLB: Dementia with Lewy bodies; ENTc: entorhinal cortex; FusG: fusiform gyrus; PD: Parkinson's disease; PDD: Parkinson's disease dementia; PHG: parahippocampal gyrus

PDD/DLB, and that parahippocampal regions show more synaptic degeneration in demented cases.

Synaptophysin and SV2A densities were both decreased in PD, PDD and DLB, but they only correlated weakly between each other. Both synaptophysin and SV2A sub-cellular localization is in synaptic vesicles at the pre-synaptic compartment [45, 46]. Our study shows that they were both more abundant in layer III than V-VI of the cortex, as expected [47], and their loss weakly associated with age, as shown before [15, 18]. However, we found a different regional distribution of the two markers: while SV2A density was higher in cortical regions affected at Braak α -synuclein stage 6 in PD(D) and DLB, synaptophysin density did not show regional density differences, which goes in line with the literature [15]. Therefore, our results suggest that even if synaptophysin and SV2A both target synaptic vesicles in the pre-synaptic compartment, they might have a differential expression or involvement in disease.

Our results indicate that NfL immunoreactivity partially contributed to regional and global synaptic loss. We previously showed that NfL accumulates in parahippocampal

regions in PDD/DLB, and that increased NfL immunoreactivity can be considered a proxy of axonal damage [29]. Increased NfL levels in biofluids are commonly used as a proxy of axonal degeneration in neurodegenerative disorders [30], but evidence of how NfL levels relate to synaptic markers is still limited. The only study investigating the correlation between regional SV2A PET binding and global CSF NfL levels did this in an AD cohort, and reported a negative correlation between NfL levels and SV2A binding in several cortical regions [48]. In line with these results, we show a coupling between regional synaptic degeneration and NfL accumulation in the brain of DLB donors, especially in regions affected at the end stage of disease, indicating that here synaptic degeneration might occur together with axonal degeneration.

We found that synaptic degeneration associated with higher LB density in parahippocampal regions affected at Braak stage 4. In physiological conditions, α -synuclein resides in the pre-synaptic compartment [12], where it might start aggregating during disease [1, 13, 14]. Previous research investigating the role of α -synuclein in cell and

animal models showed that α -synuclein overexpression led to inhibition of neurotransmitter release, by reducing the size of synaptic vesicle recycling pool [49], finally inducing synaptic failure and loss. In addition, a post-mortem study reported a negative correlation between LB density and synaptophysin levels in the occipital cortex of DLB donors [50]. In line with these results, we show that synaptic loss is more severe in cortical regions with the highest LB density, supporting the hypothesis that severe α -synuclein accumulation and aggregation contributes to synaptic degeneration.

We also addressed whether AD co-pathology contributes to cortical synaptic loss in PD, PDD, and DLB by investigating the correlations between synaptic measures, amyloid- β and p-tau load in cortical brain regions. Cortical p-tau load associations with synaptic density showed conflicting results, and did not contribute to synaptic loss in the model testing the combined contribution of all markers. We found that higher cortical SV2A density associated with higher amyloid- β load in demented donors. These findings place themselves in a complex framework based on previous literature, as there is no clear and consistent association of amyloid- β with synaptic density. In AD mouse models, both a loss [51, 52] and a clustering [52] of synaptic puncta were described at the margins of amyloid- β plaques. In our study, in order to measure synaptic puncta only within the neuropil, we excluded DAPI positive structures, which also include compact plaques [53] (Fig. S10). Therefore, our findings might relate to two phenomena: (i) a rearrangement of SV2A⁺ pre-synaptic terminals near amyloid- β plaques [52], or (ii) SV2A⁺ synapses being pushed by amyloid- β plaques in a more restricted neuropil volume. This last hypothesis is supported by a PET study in mild cognitive impairment and AD [54], which reported a strong positive correlation between hippocampal amyloid- β deposition and increased SV2A density. Taken together, our results suggest that severe amyloid- β pathology might lead to increased SV2A density, and as such PET studies using SV2A tracer should take into account AD co-pathology in patient selection and interpretation of their results.

Lastly, we showed that synaptophysin loss weakly associated with longer disease duration and worse cognition scores. Several other studies, ranging from proteomics, immunohistochemistry, CSF and PET, report correlations between synaptic degeneration, disease progression [25] and cognitive decline [16–18, 55, 56]. In line with these results, we found that synaptic loss in the cortex of PD, PDD and DLB donors partially associated with disease progression and worse cognition. In addition, we showed synaptic loss in demented donors in cortical regions near the hippocampus, which are regions known to play a central role in cognition [57]. As such, our work suggests that loss of synapses might be a correlate of cognitive decline in PD(D) and DLB, and that regional differences in synaptic loss might

partially underlie differences in cognitive status of these patients.

There are some limitations in our study. We only focused on 8 cortical regions, while several other regions, such as the substantia nigra, locus coeruleus, striatum, occipital and primary motor cortices have also shown to be affected in PD(D) and DLB [10, 23, 24]. In addition, we measured synaptic density only in pyramidal layers III and V-VI, as these layers have been shown to have the strongest loss of synaptic puncta in PD [15], therefore our results might not be representative of the whole cortical lamina. Lastly, even if we included a total of 47 brain donors, we still had small sample sizes per group (e.g. n=6 for DLB) and did not include any incidental Lewy body cases (cases with LB pathology and no PD clinical symptoms) to investigate the earliest prodromal disease stages. Therefore, future research should investigate synaptic density and its relationship to neuropathological burden in larger and more diverse cohorts.

Conclusions

Synaptic neurodegeneration occurs in temporal, cingulate and insular cortices in PD, as well as in parahippocampal regions in PDD and DLB. In addition, synaptic loss was linked to axonal damage and severe α -synuclein burden. These results together with the association of synaptic loss with disease progression and cognitive impairment, indicate that regional synaptic loss may underlie clinical heterogeneity in PD(D) and DLB. Our findings might provide useful information for the interpretation of synaptic biomarkers *in vivo*.

Abbreviations

A β	Amyloid-beta
ACC	Anterior cingulate gyrus
AD	Alzheimer's disease
AI	Anterior insula
CSF	Cerebrospinal fluid
DLB	Dementia with Lewy bodies
ENTC	Entorhinal cortex
FusG	Fusiform gyrus
GFS	Superior frontal gyrus
IHC	Immunohistochemistry
LB	Lewy body
MTG	Middle temporal gyrus
NFL	Neurofilament light chain
NFT	Neurofibrillary tangles
PCC	Posterior cingulate gyrus
PD	Parkinson's disease
PDD	Parkinson's disease dementia
PHG	Parahippocampal gyrus
p-tau	Phosphorylated-tau
pSer129- α Syn	Phosphorylated Ser129 α -synuclein

Supplementary Information

The online version contains supplementary material available at <https://doi.org/10.1186/s40478-023-01711-w>.

Supplementary Material 1: Supplementary tables

Supplementary Material 2: Supplementary figures

Supplementary Material 3: Supplementary results

Acknowledgements

We would like to thank all brain donors and their next of kin for brain donation. We would also like to thank the autopsy teams of the Netherlands Brain Bank (NBB) and Normal Aging Brain collection Amsterdam (NABCA).

Authors' contributions

I.F. contributed to experimental concept and design, data collection, statistical analysis, interpretation of the data, and drafting of the manuscript; M.M.A.B., R.T.G.M.M.N., and E.P. contributed to data collection; M.P. and E.T. supported the technical development of the synaptic imaging and analysis; A.J.M.R. contributed to the neuropathological characterization of the cohort; W.D.J.B. and L.E.J. contributed to the experimental concept and design, interpretation of the data, revised the manuscript and obtained the funding. All authors read and approved the final manuscript.

Funding

This study was funded by The Michael J. Fox Foundation (grant #17253) and Stichting ParkinsonFonds (grant #1881). The authors have no relevant financial or non-financial interests to disclose.

Declarations

Ethical approval and consent to participate

All donors signed an informed consent for brain donation and the use of material and clinical information for research purposes. The procedures for brain tissue collection of NBB and NABCA have been approved by the Medical Ethical Committee of Amsterdam UMC, Vrije Universiteit Amsterdam.

Consent for publication

Not applicable.

Availability of supporting data

Supporting data include supplementary tables, supplementary figures, and supplementary results.

Competing interests

The authors declare that they have no competing interests.

Author details

¹Department of Anatomy and Neurosciences, Section Clinical Neuroanatomy and Biobanking, Amsterdam UMC location Vrije Universiteit Amsterdam, De Boelelaan 1118, Amsterdam 1081 HV, The Netherlands

²Amsterdam Neuroscience, Neurodegeneration, Amsterdam, The Netherlands

³Amsterdam Neuroscience, Brain imaging, Amsterdam, The Netherlands

⁴Department Molecular cell biology & Immunology, Amsterdam UMC location Vrije Universiteit Amsterdam, De Boelelaan 1117, Amsterdam, Netherlands

⁵Department of Pathology, Amsterdam UMC location Vrije Universiteit Amsterdam, De Boelelaan 1117, Amsterdam, Netherlands

Received: 2 November 2023 / Accepted: 11 December 2023

Published online: 03 January 2024

References

- Bellucci A, Antonini A, Pizzi M, Spano P (2017) The end is the beginning: Parkinson's Disease in the light of brain imaging. *Front Aging Neurosci* 9:330
- Bellucci A et al (2016) Review: Parkinson's Disease: from synaptic loss to connectome dysfunction. *Neuropathol Appl Neurobiol* 42(1):77–94
- Poewe W et al (2017) Parkinson Disease. *Nat Reviews Disease Primers* 3(1):1–21
- Aarsland D, Zuccai J, Brayne C (2005) A systematic review of prevalence studies of Dementia in Parkinson's Disease. *Mov Disorders: Official J Mov Disorder Soc* 20(10):1255–1263
- Jellinger KA (2022) Morphological basis of Parkinson disease-associated cognitive impairment: an update. *J Neural Transm* 1–23
- e Sousa CS, Alarcão J, Martins IP, Ferreira JJ (2022) Frequency of Dementia in Parkinson's Disease: a systematic review and meta-analysis. *J Neurol Sci* 432:120077
- Emre M et al (2007) Clinical diagnostic criteria for Dementia associated with Parkinson's Disease. *Mov Disorders: Official J Mov Disorder Soc* 22(12):1689–1707
- McKeith IG et al (2017) Diagnosis and management of Dementia with Lewy bodies: fourth consensus report of the DLB Consortium. *Neurology* 89(1):88–100
- Jellinger KA (2003) Neuropathological spectrum of synucleinopathies. *Mov Disorders: Official J Mov Disorder Soc* 18(S6):2–12
- Braak H et al (2003) Staging of brain pathology related to sporadic Parkinson's Disease. *Neurobiol Aging* 24(2):197–211
- Shahmoradian SH et al (2019) Lewy pathology in Parkinson's Disease consists of crowded organelles and lipid membranes. *Nat Neurosci* 22(7):1099–1109
- Burré J (2015) The synaptic function of α -synuclein. *J Parkinson's Disease* 5(4):699–713
- Longhena F et al (2017) *The contribution of α -synuclein spreading to Parkinson's disease synaptopathy* Neural plasticity, 2017
- Longhena F, Faustini G, Spillantini MG, Bellucci A (2019) Living in promiscuity: the multiple partners of alpha-synuclein at the synapse in physiology and pathology. *Int J Mol Sci* 20(1):141
- Zhan S-S, Beyreuther K, Schmitt H (1993) Quantitative Assessment of the Synaptophysin Immuno-Reactivity of the cortical neuropil in various neurodegenerative disorders with Dementia. *Dement Geriatr Cogn Disord* 4(2):66–74
- Berezcki E et al (2018) Synaptic markers of cognitive decline in neurodegenerative Diseases: a proteomic approach. *Brain* 141(2):582–595
- Berezcki E et al (2016) Synaptic proteins predict cognitive decline in Alzheimer's Disease and Lewy body Dementia. *Alzheimer's Dement* 12(11):1149–1158
- Berezcki E et al (2017) Synaptic proteins in CSF relate to Parkinson's Disease stage markers. *Npj Parkinson's Disease* 3(1):1–5
- Chatterjee M et al (2020) Contactin-1 is reduced in cerebrospinal fluid of parkinson's Disease patients and is present within lewy bodies. *Biomolecules* 10(8):1177
- Lerche S et al (2021) CSF protein level of neurotransmitter secretion, synaptic plasticity, and autophagy in PD and DLB. *Mov Disord* 36(11):2595–2604
- Nilsson J et al (2023) Cerebrospinal fluid biomarkers of synaptic dysfunction are altered in Parkinson's Disease and Related disorders. *Mov Disord* 38(2):267–277
- Mercier J, Provins L, Valade A (2017) Discovery and development of SV2A PET tracers: potential for imaging synaptic density and clinical applications. *Drug Discovery Today: Technologies* 25:45–52
- Matuskey D et al (2020) Synaptic changes in Parkinson Disease assessed with in vivo imaging. *Ann Neurol* 87(3):329–338
- Andersen KB et al (2021) Reduced synaptic density in patients with Lewy Body Dementia: an [11 C] UCB-J PET imaging study. *Mov Disord* 36(9):2057–2065
- Wilson H et al (2020) Mitochondrial complex 1, sigma 1, and synaptic vesicle 2A in early drug-naive Parkinson's Disease. *Mov Disord* 35(8):1416–1427
- Hepp DH et al (2016) Distribution and load of amyloid- β pathology in Parkinson Disease and Dementia with Lewy bodies. *J Neuropathology Experimental Neurol* 75(10):936–945
- Irwin DJ et al (2017) Neuropathological and genetic correlates of survival and Dementia onset in synucleinopathies: a retrospective analysis. *Lancet Neurol* 16(1):55–65
- Irwin DJ et al (2012) Neuropathologic substrates of Parkinson Disease Dementia. *Ann Neurol* 72(4):587–598
- Frigerio I et al (2023) Neurofilament light chain is increased in the parahippocampal cortex and associates with pathological hallmarks in Parkinson's Disease Dementia. *Translational Neurodegeneration* 12(1):3
- Ashton NJ et al (2021) A multicentre validation study of the diagnostic value of plasma neurofilament light. *Nat Commun* 12(1):1–12
- Jonkman LE et al (2019) Normal aging brain Collection Amsterdam (NABCA): a comprehensive collection of postmortem high-field imaging, neuropathological and morphometric datasets of non-neurological controls, vol 22. *Clinical, Neurolmage*, p 101698

32. Postuma RB et al (2015) MDS clinical diagnostic criteria for Parkinson's Disease. *Mov Disord* 30(12):1591–1601
33. Morris JC (1991) The clinical Dementia rating (cdr): current version and. *Young* 41:1588–1592
34. Alafuzoff I et al (2009) Assessment of β -amyloid deposits in human brain: a study of the BrainNet Europe Consortium. *Acta Neuropathol* 117(3):309–320
35. Alafuzoff I et al (2008) Staging of neurofibrillary pathology in Alzheimer's Disease: a study of the BrainNet Europe Consortium. *Brain Pathol* 18(4):484–496
36. Alafuzoff I et al (2009) Staging/typing of Lewy body related α -synuclein pathology: a study of the BrainNet Europe Consortium. *Acta Neuropathol* 117(6):635–652
37. Morales J et al (2013) Characterization and extraction of the synaptic apposition surface for synaptic geometry analysis. *Front Neuroanat* 7:20
38. Bankhead P et al (2017) QuPath: open source software for digital pathology image analysis. *Sci Rep* 7(1):16878
39. Arendt T et al (2017) Inhomogeneous distribution of Alzheimer pathology along the isocortical relief. Are cortical convolutions an Achilles heel of evolution? *Brain Pathol* 27(5):603–611
40. Frigerio I et al (2021) Amyloid- β , p-tau and reactive microglia are pathological correlates of MRI cortical atrophy in Alzheimer's Disease. *Brain Commun* 3(4):fcab281
41. Montine TJ et al (2012) National Institute on Aging–Alzheimer's Association guidelines for the neuropathologic assessment of Alzheimer's Disease: a practical approach. *Acta Neuropathol* 123(1):1–11
42. Thal DR, Rüb U, Orantes M, Braak H (2002) Phases of A β -deposition in the human brain and its relevance for the development of AD. *Neurology* 58(12):1791–1800
43. Braak H et al (2006) Staging of Alzheimer disease-associated neurofibrillary pathology using paraffin sections and immunocytochemistry. *Acta Neuropathol* 112(4):389–404
44. Thal DR et al (2002) Two types of sporadic cerebral amyloid angiopathy. *J Neuropathol Exp Neurol* 61(3):282–293
45. Calakos N, Scheller RH (1994) Vesicle-associated membrane protein and synaptophysin are associated on the synaptic vesicle. *J Biol Chem* 269(40):24534–24537
46. Stout KA, Dunn AR, Hoffman C, Miller GW (2019) The synaptic vesicle glycoprotein 2: structure, function, and Disease relevance. *ACS Chem Neurosci* 10(9):3927–3938
47. Palomero-Gallagher N, Zilles K (2019) Cortical layers: Cyto-, myelo-, receptor- and synaptic architecture in human cortical areas. *NeuroImage* 197:716–741
48. Mecca AP et al (2020) Association between cerebrospinal fluid biomarkers of neurodegeneration and PET measurements of synaptic density in Alzheimer's Disease: Neuroimaging/multi-modal comparisons, vol 16. *Alzheimer's & Dementia*, p e044211
49. Nemani VM et al (2010) Increased expression of α -synuclein reduces neurotransmitter release by inhibiting synaptic vesicle recluster after endocytosis. *Neuron* 65(1):66–79
50. Mukaetova-Ladinska EB et al (2013) Synaptic proteins and choline acetyltransferase loss in visual cortex in Dementia with Lewy bodies. *J Neuropathology Experimental Neurol* 72(1):53–60
51. Koffie RM et al (2009) *Oligomeric amyloid β associates with postsynaptic densities and correlates with excitatory synapse loss near senile plaques* Proceedings of the National Academy of Sciences, 106(10): p. 4012–4017
52. Dong H, Martin MV, Chambers S, Csernansky JG (2007) Spatial relationship between synapse loss and β -amyloid deposition in Tg2576 mice. *J Comp Neurol* 500(2):311–321
53. Mabrouk R, Gotkiewicz M, Rauramaa T, Tanila H (2022) DAPI (4', 6-diamidino-2-phenylindole) stains Compact amyloid plaques. *J Alzheimers Dis Preprint*:1–7
54. O'Dell RS et al (2021) Association of A β deposition and regional synaptic density in early Alzheimer's disease: A PET imaging study with [11 C], vol 13. *UCB-J. Alzheimer's Research & Therapy*, pp 1–12
55. Head E et al (2009) Synaptic proteins, neuropathology and cognitive status in the oldest-old. *Neurobiol Aging* 30(7):1125–1134
56. Terry RD et al (1991) Physical basis of cognitive alterations in Alzheimer's Disease: synapse loss is the major correlate of cognitive impairment. *Annals of Neurology: Official Journal of the American Neurological Association and the Child Neurology Society* 30(4):572–580
57. Weintraub D et al (2011) Neurodegeneration across stages of cognitive decline in Parkinson Disease. *Arch Neurol* 68(12):1562–1568

Publisher's Note

Springer Nature remains neutral with regard to jurisdictional claims in published maps and institutional affiliations.